ICARUS **130,** 57–67 (1997)
ARTICLE NO. IS975813

Mid-to-Low Latitude H_3^+ Emission from Jupiter

Steven Miller and Nicholas Achilleos

Department of Physics and Astronomy, University College London, Gower Street, London WC1E 6BT, United Kingdom
E-mail: s.miller@ucl.ac.uk

Gilda E. Ballester

Department of Atmospheric, Oceanic and Space Sciences, University of Michigan, 2455 Hayward, Ann Arbor, Michigan 48109

Hoanh An Lam and Jonathan Tennyson

Department of Physics and Astronomy, University College London, Gower Street, London WC1E 6BT, United Kingdom

Thomas R. Geballe

Joint Astronomy Centre, 660 N A'ohoku Place, Hilo, Hawaii 96720

and

Laurence M. Trafton

Department of Astronomy and McDonald Observatory, University of Texas at Austin, Austin, Texas 78712

Received April 21, 1997; revised July 9, 1997

We present measurements of the mid-to-low latitude H_3^+ emission from Jupiter, derived from a spectroscopic study of the planet carried out on the United Kingdom Infrared Telescope (UKIRT) on Mauna Kea, Hawaii, on May 3–5, 1993. The measurements indicate ionospheric H_3^+ temperatures ~800 K and column densities of the order of 10^{11} cm^{-2}. The emission levels depend strongly on latitude and longitude, but are generally of the order of 10^{-1} erg s^{-1} cm^{-2}, indicating that the cooling effect of H_3^+ is a significant factor in the ionosphere. These emission levels also strongly suggest either that aurorally produced $H_3^+$is being transported to nonauroral latitudes or that sources in addition to solar EUV are required to produce the ionisation and excitation energy necessary to account for the observed H_3^+ emission. This view is supported by comparing the emission profiles as a function of latitude with those obtained from a jovian global circulation model which has auroral electron precipitation and solar EUV as ionisation inputs. The spatial distribution of H_3^+ emission suggests that this ion may be a useful probe of Jupiter's magnetic field at subauroral latitudes.

1. INTRODUCTION

The importance of the H_3^+ molecular ion as a constituent of the jovian ionosphere has long been recognized by workers modeling the atmospheres of the outer planets (see, e.g., Atreya and Donahue, 1976). The Voyager II spacecraft detected an ion with a mass:charge ratio of 3:1 in Jupiter's magnetosphere during its flyby of the planet in 1979 (Hamilton *et al.*, 1980). Since its spectroscopic detection in the jovian aurorae in 1988 (Drossart *et al.*, 1989), H_3^+ emission has been used to probe auroral activity and morphology using both spectroscopic and imaging techniques (see review by Miller *et al.*, 1994, and references therein). In recent years a number of infrared spectroscopic studies of Jupiter have shown that emission from the fundamental rovibrational band of the H_3^+ molecular ion may be detected from all parts of the planetary disk (Miller *et al.*, 1992; de Bergh *et al.*, 1992; Ballester *et al.*, 1994, henceforth Paper I). This gave rise to the expectation that H_3^+ emission could be used to probe and monitor conditions in the nonauroral ionosphere. Paper I, for instance, considered a potential link between H_3^+ emission and the Lyman-α Bulge, a region around Jupiter's equator which shows enhanced Lyman-α emission. Also, during the collision of Comet Shoemaker–Levy 9 with Jupiter in July 1994, several groups studied the effects of the impacts on the ionosphere by monitoring this ion (Dinelli *et al.*, 1997; Kim *et al.*, 1996; Schultz *et al.*, 1995).

0019-1035/97 $25.00

Recently, we have published results from a study of jovian H_3^+ emission carried out on the United Kingdom Infrared Telescope (UKIRT) on Mauna Kea, Hawaii, on May 3–5, 1993 (Lam *et al.*, 1997, henceforth Paper II). While this paper concentrated on the auroral H_3^+ emission, some details of nonauroral emission were also included. In general, Paper II explained that H_3^+ emission is produced by the radiative relaxation of collisionally excited ions, which exist in a state of "quasi-LTE." The emission, especially in the mid-to-low latitude regions, is generally optically thin. Paper II also introduced a parameter $E(H_3^+)$, which allowed for the strong coupling between fitted temperatures and column densities. This parameter is defined by calculating the total emission per molecule at the appropriate fitted temperature, assuming local thermal equilibrium, and multiplying it by the corresponding fitted column density. (For further discussion of the reliability of this parameter, see Paper II.) $E(H_3^+)$ is particularly useful for the subauroral latitude study, where emission levels are relatively weak and spectra rather noisy, and where we are forced to use a rather assorted selection of H_3^+ spectral lines for the purposes of fitting.

In this paper, we examine the behavior of subauroral H_3^+ in terms of temperature and column density variations, the resulting planetary distribution of $E(H_3^+)$, and what this means in terms of the energy balance in the ionosphere. We compare the observed H_3^+ variation with latitude with that predicted by a jovian global circulation model (JIM, Achilleos *et al.*, 1997).

2. DATA ACQUISITION AND ANALYSIS

All data were obtained with UKIRT's long slit grating spectrometer; full details of the UKIRT data acquisition and reduction have already been given in Papers I and II, and only the essential details are recapped here. This present study is based solely on the CGS4 spectra obtained in the wavelength range 3.37–3.57 μm (central wavelength 3.47 μm) and with the slit aligned north–south along the jovian central meridian longitude (CML). Times and central longitudes observed are given in Table 1. Each spectrum consisted of 2.4 min of exposure time on Jupiter and 2.4 min on adjacent sky (to remove the sky background from Jupiter) and took ~6 min to complete (corresponding to a jovian rotation of 3.6°). The pixel size was 3.08″ × 3.08″, corresponding to ~10,000 × 10,000 km on a plane at the distance to Jupiter. The pixel thus subtended ~8.0° of longitude × ~8.2° of latitude at the sub-Earth point, rising to ~12.5° of longitude × ~13.1° of latitude at a sub-Earth point of ±50° along the CML. Since all the data used in Papers I and II and this paper were obtained with the spectrometer slit aligned along the CML, they refer to the planetary local noon. This observing strategy was adopted in order to concentrate on longitudinal and latitudinal variations, while eliminating local time effects. As discussed in Paper II, temporal variations also play a part in determining the H_3^+ emission spectrum. But comparison of Tables 2 (CML 324°, May 3, 1993) and 3 (CML 325°, May 5, 1993) of Paper II shows that this is not too great a problem to prohibit using data obtained at different times to build up a picture of the spatial variation of the jovian H_3^+ emission. This is particularly so in the mid-to-low latitudes discussed here, where temperatures at equivalent locations throughout the region vary within the stated errors on the two days, and the more significant $E(H_3^+)$ profiles are within 10% of each other at all non-auroral latitudes.

TABLE 1
UKIRT 3.47-μm Data Obtained during 1993

Date	Time (U.T.)	CML (System III)
May 3	05:36	102
	07:42	180
	08:32	210
	09:46	254
	11:37	324
May 4	05:14	241
	07:33	325
	08:55	40
May 5	05:42	47
	09:11	174

TABLE 2
Comparison of 1992 and 1993 Data Obtained at CML = 102°

1992 data			1993 data		
Position (Lat/km)	T(K)	$N(H_3^+)$ (10^{12} cm^{-2})	Position (Lat/km)	T(K)	$N(H_3^+)$ (10^{12} cm^{-2})
8000[a]	819	0.13	10,484[a]	1053	0.15
3000[a]	869	0.81	183[a]	822	5.42
N 67°	706	6.71	N 56°	639	3.01
N 48°	664	1.78	N 42°	763	0.21
N 36°	983	0.19	N 30°	823	0.10
N 25°	1043	0.14	N 21°	761	0.12
N 15°	1250	0.08	N 12°	976	0.05
N 06°	1100	0.10	N 04°	761	0.15
S 01°	1140	0.10	S 04°	813	0.12
S 09°	829	0.28	S 12°	764	0.20
S 18°	1230	0.07	S 21°	741	0.24
S 28°	1140	0.10	S 30°	752	0.32
S 39°	863	0.22	S 42°	803	0.45
S 51°	827	1.29	S 56°	943	0.81
S 75°	900	5.00	183[a]	786	4.40
3000[a]	680	11.54	10,484[a]	764	0.13

[a] Distances in kilometers above the limb of the planet, determined by fitting program (see Paper II).

Details of the method of analysis of the data have also largely been given in Papers I and II. There is, however, an important difference between Paper I and the current study in the handling of the background continuum emission. At 3.47 μm, much of the solar infrared radiation incident at Jupiter is absorbed by the ν_3 band of methane, present in the stratosphere with a mixing ratio $\sim 10^{-3}$. To a first approximation, the absorbing column is enhanced along the line of sight by a factor of $1/\cos(\phi)$, where ϕ is the local solar zenith angle (equivalent to the latitude, since our observations were made with the slit aligned along the CML). As a result, in the auroral regions—and at higher latitudes generally—very little background radiation is seen in moderate resolution spectra. Since the H_3^+ emission is generally much greater (typically up to 50 times) than the continuum, the effect of the background on fitted temperatures and column densities is negligible. But at latitudes close to the equator, the intensity of the continuum reflected solar IR is greater, since the absorbing methane column is less than towards the poles, and the H_3^+ emission up to 50 times weaker than in the auroral regions. As a result, the continuum may be up to 25% of the line intensity. Clearly then, the treatment of this continuum in fitting the mid-to-low-latitude spectra may significantly affect the values for temperature and column density derived. Paper I assumed that this could be approximated by a constant across the entire wavelength region ($\sim$0.25 μm). During the course of this study, however it became clear that this treatment, adopted for the 1992 data because of their rather poor signal-to-noise level, was an oversimplification.

The background in the 3.47 μm spectral window could have structure if there were absorption features in the incident solar radiation or as a result of differential absorption by jovian stratospheric methane; Drossart *et al.* (1996) have recently ascribed one feature at 3.52 μm (see Fig. 2, Paper II) to the latter effect. Solar absorption features are at the level of a few percent of the solar continuum emission—and therefore about 1% of the peak intensities of our spectra, when scaled to the background level (maximum 25% of the line intensity), well within the noise of our data—throughout the spectral range of interest, with the exception of one unidentified line at 3.523 μm and lines due to silicon and magnesium between 3.396 and 3.400 μm (Livingstone and Wallace, 1994). Fortunately, none of these coincide with any of the strong H_3^+ emission features used in fitting the data presented here. For simplicity, we did not use a line-by-line calculation of the absorption due to jovian stratospheric methane, since our primary concern in this study was the emission due to H_3^+. In the present study, therefore, the H_3^+ lines were first manually removed from the spectrum and the resulting background between the lines was fitted by a low-order polynomial. This background was then smoothly extrapolated under the H_3^+ line positions, giving an estimate of the continuum emission of accuracy appropriate to the signal-to-noise ratio and the temperature/column density fitting procedure. The effect of this improved background estimation on the 1992 data is discussed in the next section.

3. H_3^+ TEMPERATURE AND COLUMN DENSITY

Typical fitted H_3^+ temperatures and column densities are given in Tables 2 and 3 of Paper II. They show that outside of the bright auroral regions, derived temperatures ranged from below 700 K (as low as 639 K in one instance) to around 850 K (up to 875 K, in another), with 2σ errors between $\pm$10 and $\pm$15%. Column densities prior to line-of-sight correction ranged from values near the equator around 1×10^{11} cm^{-2} to up to six times that value at the higher latitudes ($\sim \pm 50°$), with errors of $\pm$55% at the equator falling to around $\pm$20% at higher latitudes.

In Table 2 we compare the results obtained in Paper I, which is based on 1992 data and fitted with a constant background, with those derived in the present study, where we also made measurements at CML = 102° in 1993, and fitted them with a background produced as described above. Paper I reported that there was a temperature enhancement of $\sim$200–300 K in the fitted equatorial temperatures of the 1992 dataset compared with that derived for the auroral regions. Dividing the planet as a whole into three regions to improve the statistics of the data (particularly in the central latitudes), they found a temperature of 1220 $\pm$ 120 K in the central region (latitudes +30°–−33°), compared with 813 $\pm$ 41 K in the southern higher latitude region and 734 $\pm$ 37 K in the northern. Among other things, the authors of Paper I considered that their results could provide support for a new explanation for the Lyman-α Bulge proposed by Ben Jaffel *et al.* (1992) and later extensively modeled by Sommeria *et al.* (1995). These models suggested enhanced temperatures as a result of strong winds flowing from the auroral regions.

The 1993 results, however, indicate less spatial variability in temperature than was suggested by Paper I. We now consider that the higher central region temperatures obtained in that paper were an artifact which resulted from an inadequate treatment of the continuum background radiation, particularly at shorter wavelengths. This resulted in the higher energy H_3^+ lines having their intensity artificially enhanced, hence apparently increasing the fitted temperature. The 1992 data are noisier that that of 1993, however, and reliably fixing the background was consequently more difficult and the fit less reliable. This meant that reanalysis of individual rows, using backgrounds determined in the same way as for the 1993 data, gave uncertainties too large to make the results useful. But it was possible to reanalyze combined rows of the central region. This

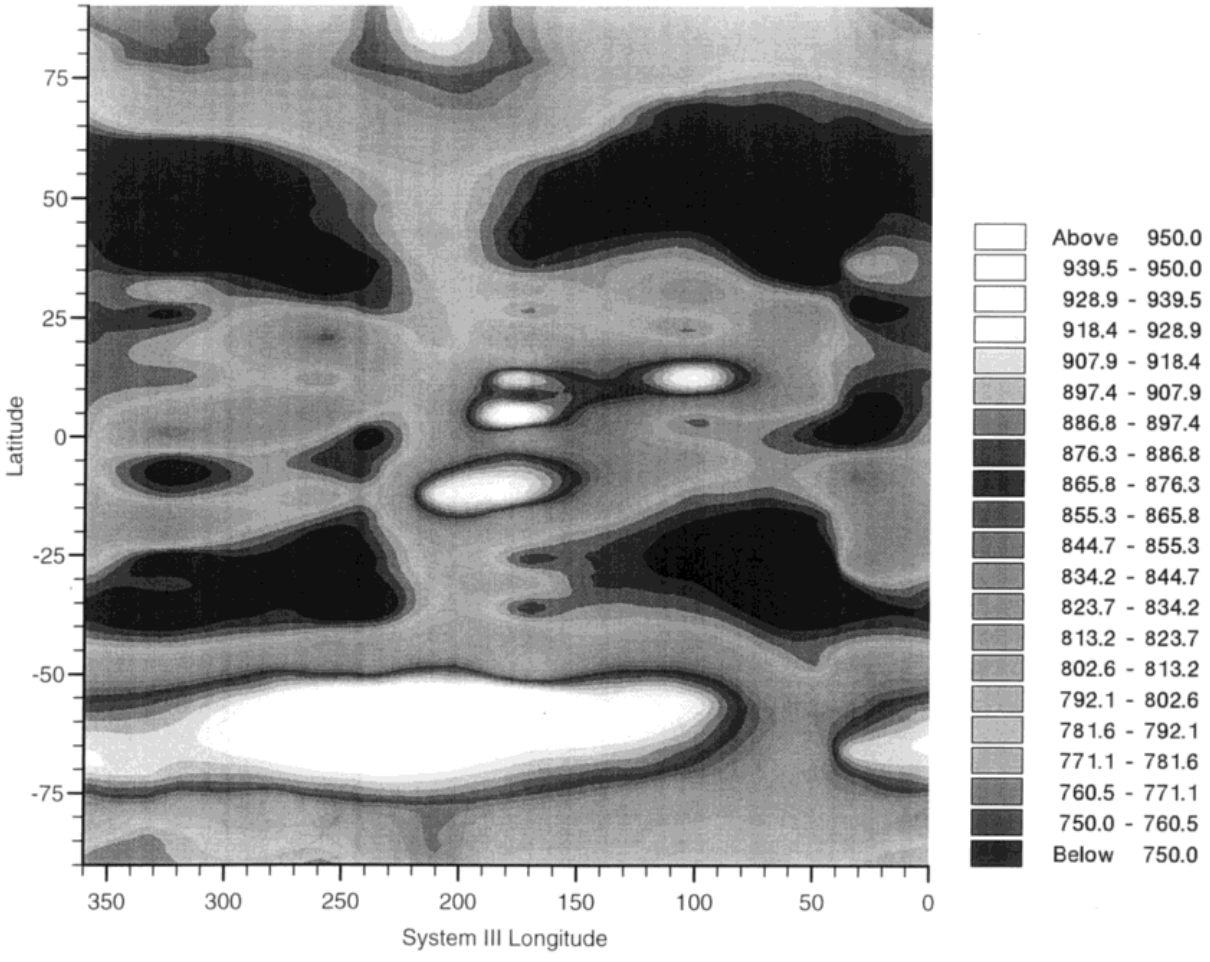

FIG. 1. Global jovian H_3^+ temperature distribution.

produced a mid-to-low-latitude temperature for the central region (latitudes $+30°$–$-33°$) of 930($+150/-110$) K, considerably lower than 1220 (± 120) K reported in Paper I. Nonetheless, as will be seen below, it does seem as if there is some coincidence between the pattern of H_3^+ emission and the location of the Lyman-α Bulge. Although there may be a physical connection between the phenomena, this coincidence may be also fortuitous.

In Figs. 1 and 2, the fitted results for temperature and column density, corrected for line-of-sight effects, are presented as a function of planetary location. (As reported in Paper II, at the mid-to-low latitudes discussed here, the line-of-sight correction was approximated by a secant effect.) Contours between the datapoints were interpolated using a two-dimensional spline interpolation with the Uniras graphics package. A moderate stiffness of 4 (stiffnesses anywhere between 3 and 5 made little difference to the overall plot) was chosen to trace real point-to-point variations without introducing spurious features. (A stiffness of 2 or below allowed too much flexibility in the plotting and produced interpolation artifacts; stiffnesses of 7–9 were so large as to completely override genuine spatial variations.) The maps were produced from the full 1993 dataset, which includes data taken at a central wavelength of 4.00 μm. However, for reasons explained in Paper II, the 4 μm data only cover the auroral regions. (The full dataset is still useful for mid-to-low-latitude regions since the periauroral values derived at 4 μm help constrain the overall plot and fill in some of the gaps.) As a result, there are some gaps in the data at mid-to-low latitudes, particularly between System III longitudes $\lambda_{III} = 102°$ and 174°, and between $\lambda_{III} = 325°$ and $\lambda_{III} = 40°$. The spatial resolution of the pixels, given in Section 2, and the ''smearing'' due to the 3.6° planetary rotation during each 6-min exposure, must also be taken into account. Thus some of the small-scale mid-to-low-latitude detail produced in the figures may still be a product of program interpolation between the datapoints. Outside of the auroral regions, therefore, the data

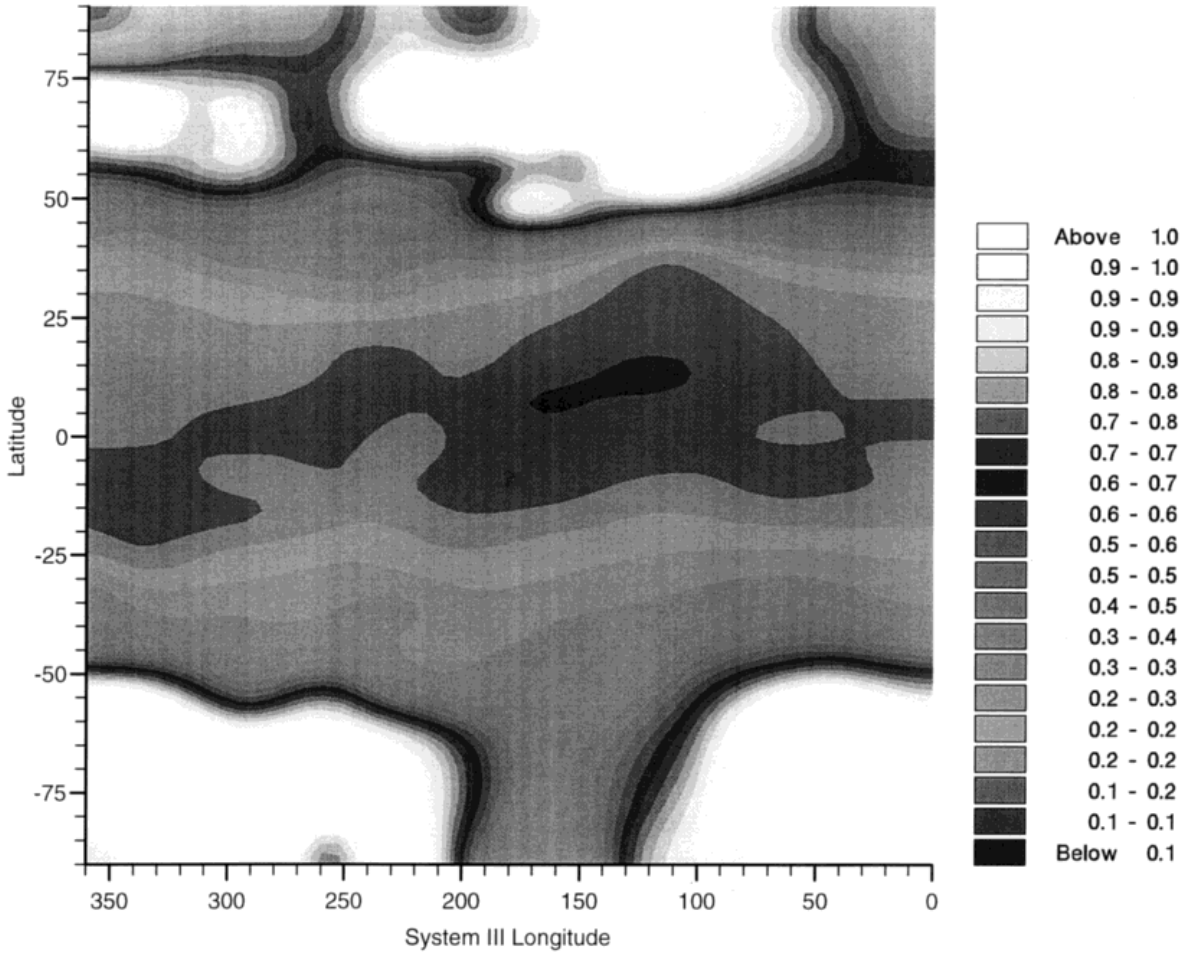

FIG. 2. Global jovian H_3^+ column density distribution in units of 10^{12} cm^{-2}. (Corrections for line of sight effects have been made.)

should be used to derive trends rather than indicate specific local knowledge.

In the mid-to-low-latitudes, our data show that there is a tendency for the temperature to fall from around 850–950 K, close to the auroral regions, to between 700 and 800 K in regions centered on N 40° and S 35°. But toward the equator, the temperature does appear to climb, once more, closer to the near-auroral 850–950 K range. In addition, there appears to be a warm channel linking the northern and southern auroral regions centered around λ_{III} = 170°–210°, a region reasonably well sampled by our dataset. This channel could possibly extend to lower longitudes where we do not have coverage in the mid-to-low-latitude region, although the mapping is somewhat constrained by auroral and periauroral 4 μm data at λ_{III} = 160° (Table 1 of Paper II). The column density map shows rather less latitudinal structure than the temperature map. Densities fall from a maximum of $\sim$1.0 $\times$ 10^{12} cm^{-2} at latitudes around 55° to below 0.1 $\times$ 10^{12} cm^{-2} at the equator.

4. H_3^+ TOTAL EMISSION, $E(H_3^+)$

As explained in Paper II, the derived column densities and temperatures are strongly anticorrelated, and the values resulting from our fitting procedure may cover a large range of parameter space (see Fig. 6 of Paper II), giving rise to large errors in the individual parameters. As a result, a new parameter $E(H_3^+)$ was introduced. This parameter gives a value for the total emission due to the H_3^+ ion, derived by combining the fitted temperatures and column densities, and assuming LTE. Paper II showed that this parameter has associated errors of $\pm$20% to $\pm$25% for the mid-to-low-latitude regions.

$E(H_3^+)$ is a useful parameter as it gives the cooling rate for this important constituent of the jovian ionosphere. Outside the auroral regions, the value of $E(H_3^+)$ (after line-of-sight correction) varies between 0.2 and 0.5 ergs s^{-1} cm^{-2} at latitudes around 40°, down to 0.05 to 0.10 ergs s^{-1} cm^{-2} around the equator. These levels are higher than had

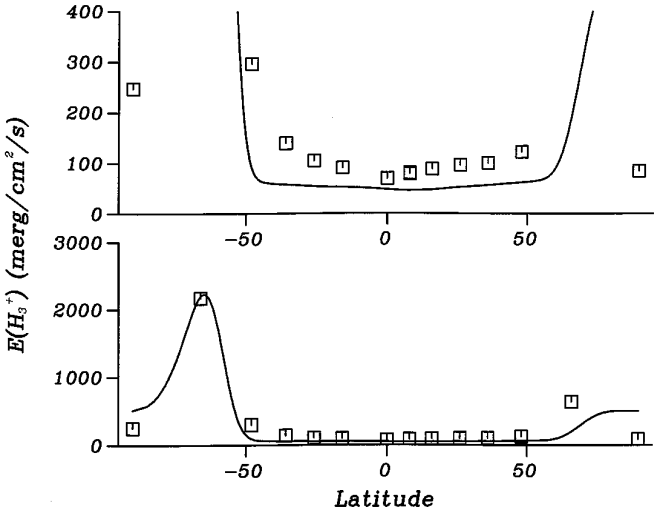

FIG. 3. Comparison of jovian H_3^+ emission, $E(H_3^+)$, profile at $\lambda_{III} = 40°$ predicted by the JIM global circulation model with that derived from the 1993 dataset. Squares: data points. Solid curve: JIM profile convolved with CGS4 spatial resolution. (No line of sight corrections have been made.)

previously been considered. At the equator the total jovian H_3^+ line flux is comparable to the incident flux of solar EUV (Lean, 1987)—a point we shall return to later. Recent modeling by Waite *et al.* (1997), making use of the cooling rates published here (first reported in Lam, 1995), has shown that inclusion of cooling due to H_3^+ considerably alters the thermal structure of the nonauroral ionosphere.

In Fig. 3, we compare the latitudinal profile of $E(H_3^+)$ with that predicted by a jovian ionospheric model (JIM, Achilleos *et al.*, 1997). The exact details of the model are not relevant to this study, except insofar as JIM is a three-dimensional global circulation model which allows for coupling between different latitudes and longitudes via self-consistently generated winds. Calculations are carried out on a grid of 2° in latitude and 9° in longitude. Currently, the energy inputs to the model of importance to this study are (i) electron precipitation of 10 keV at 8 ergs s^{-1} cm^{-2} confined between the footprints of the Io Plasma Torus and field lines (as predicted by the O6 plus current sheet model of Connerney (1993)) which correlate to the magnetospheric region in which plasma corotation breaks down; (ii) approximately 4×10^{-2} erg s^{-1} cm^{-2} of H-ionizing solar EUV radiation incident at the subsolar point on the planet's atmosphere, with ~50% of the total contributing to ionospheric heating (consistent with Atreya, 1986); and (iii) standard jovian ionospheric chemistry (e.g., Strobel and Atreya, 1983). The current restrictions of the model which are relevant to this study are (i) that the auroral energy input is more dispersed than the latest imaging would suggest is appropriate (Clarke *et al.*, 1996); thus (ii) the model does not generate supersonic auroral winds; and (iii) no particle precipitation outside of the auroral region is included. With these restrictions the model predicts that at latitudes immediately adjacent to the auroral regions, where only the effect of solar EUV is present, the H_3^+ emission (before line-of-sight correction) should fall rapidly toward its minimum value at the equator. This is not, however, what is observed in the data. Instead, the observations show that $E(H_3^+)$ decreases much more slowly as a function of decreasing latitude, and that the model seriously underestimates the intensity close to the auroral regions. We shall also return to this point later.

In Fig. 4, we present mid-to-low latitude details of the $E(H_3^+)$ map (corrected for line-or-sight effects) presented as Fig. 7 of Paper II. The figure indicates that, superimposed on the general tendency for $E(H_3^+)$ to fall with decreasing latitude, there are considerable longitudinal variations. The first point to note is that the minimum in the H_3^+ emission does not always coincide with the equator. In particular, there appears to be a region between $\lambda_{III} = 60°$ and 170° where the minimum is as much as 20° north of the equator. (The region between $\lambda_{III} = 102°$ and 174° is not sampled in the mid-to-low latitudes.) Other longitudinal regions have emission minima which differ from the rotational equator by lesser, though not insignificant, amounts.

It is also noteworthy that, although the present study does not support temperatures as high as 1200 K associated with the Lyman-α bulge, insofar as our dataset samples it, this feature does appear to coincide with a region of relatively elevated temperatures (Fig. 1) and with the region of least H_3^+ emission. This emission minimum results from the lower column densities which accompany the elevated temperatures, raising once more the possibility suggested in Paper I that the emission in this region is being produced by H_3^+ produced at higher altitudes than in the auroral regions, i.e., closer to the nanobar than the 0.1 microbar level, a point to which we return later. The warm channel linking the northern and southern auroral regions around $\lambda_{III} = 170–210°$, noted above, also shows up as a region of brighter emission reaching (almost) right across the equator.

5. CANDIDATE EXPLANATIONS FOR THE OBSERVED H_3^+ EMISSION

The results outlined above show that the H_3^+ molecular ion is to be found in the mid-to-low-latitude regions in concentrations sufficient for it to radiate away a considerable fraction of the energy received by Jupiter's upper atmosphere. But standard discussions (e.g., Atreya, 1986) indicate that there is too little incident solar EUV to account for the observed H_3^+ densities and emission, if the ion is being produced and excited *in situ*. It is therefore important to understand the mechanisms by which H_3^+ is

being transported to or produced in the planetary locations where it is found.

5.1. Transport Processes

One way of producing high H_3^+ concentrations (and thus emissions) in the mid-to-low latitudes could be to transport it there from the auroral regions where it is produced in high concentrations. According to Atreya (1986), were the auroral energy of Jupiter to be evenly and efficiently spread across the entire planetary disk, it would amount to 0.4 erg s^{-1} cm^{-2}, and would thus be more than enough to account for the H_3^+ emission in the mid-to-low latitudes. Waite *et al.* (1983) suggested that this "distributive" process might be achieved by strong thermospheric winds. They showed that diluting the auroral energy in this way produced temperature profiles in agreement with those deduced by Voyager.

The impact of Comet Shoemaker–Levy 9 on Jupiter in July 1994 enabled planetary astronomers to obtain values for a number of important parameters concerned with the jovian atmosphere. One of importance to this study is the speed of meridional winds in the upper atmosphere. Clarke *et al.* (1995) showed that the spread of the impact sites could be accounted for by winds in the upper stratosphere of between 30 and 50 m s^{-1}. This value was shown to be consistent with the timescale involved with the quenching of the southern aurora (Miller *et al.*, 1995), presumably due to the transport of material in the lower ionosphere, and with the 10–100 nanobar wind speeds predicted by JIM (Achilleos *et al.*, 1997). While such winds might transport energy efficiently, however, they could not account for the observed distribution of H_3^+ densities away from the auroral regions. The dissociative recombination coefficient for the reaction of H_3^+ with electrons remains controversial but is now generally thought to be approximately 10^{-7} cm^3 s^{-1} (Mitchell, 1990, and private communication). At electron densities typical of the auroral regions where it is produced ($[e^-] = 10^4$–10^5 cm^{-3} at 0.1 μbar), H_3^+ lifetimes are therefore between 100 and 1000 s. Thus velocities in excess of 10 km s^{-1}, rather than the $<$100 m s^{-1} which seems probable in the upper stratosphere/lower ionosphere, are required to transport the ion the tens of thousands of kilometers away from the auroral regions to where it is observed.

Wind speeds suggested by Sommeria *et al.* (1995) are, on the other hand, much greater than this—of the order of 10 km s^{-1}. However, these winds are being produced at high altitudes (in the nanobar region) where models (e.g., Atreya and Donahue, 1976; McConnell and Majeed, 1991) predict that H_3^+ is being produced in the auroral regions at much lower concentrations than at the 0.1 microbar production peak. One is left with the conclusion that, at altitudes where wind speeds may be sufficient to transport H_3^+ from the aurorae to lower latitudes, the concentration is too low to account for the mid-to-low latitude concentrations observed, and where the auroral production rates are high, the lifetimes and wind speeds are too low. The failure of JIM to reproduce the observed latitudinal distribution, using just auroral particle precipitation, horizontal subsonic winds, and solar EUV, supports this.

It is, however, possible that auroral H_3^+ produced at the 0.1 μbar level is being vertically transported to the nanobar level, where it is then being dispersed to lower latitudes. (At present, vertical winds in the JIM model are computed using hydrostatic equilibrium in the vertical direction, rather than an independent momentum transfer equation.) Sommeria *et al.*'s (1995) model indicates that the transit time from the auroral regions to the equator is less than 10^4 s. In the nanobar region, electron densities are typically $\sim 10^2$ cm^{-3} and would allow H_3^+ lifetimes of 10^4 to 10^5 s, enough time for it to be transported across the entire planet. Recently, evidence of vertical transport has been observed in auroral Lyman-α emissions (Prangé *et al.* 1997). Another contribution to the transport of energy, and hence H_3^+, from the auroral to subauroral regions may be due to the presence of long-lived H^+ and small amounts of He^+. This latter ion may be formed by particle precipitation and has a recombination rate with electrons of $\sim 10^{-11}$ cm^3 s^{-1}, giving it a lifetime of at least 10^6 s even at the 0.1 μbar level. It reacts slowly with H_2, with a rate of $\sim 10^{-13}$ cm^3 s^{-1}, giving rise to products such as HeH^+ and H_2^+, both of which form H_3^+ (Roberge and Dalgarno, 1982). At the nanobar level, where $[H_2]$ is between 10^{10} and 10^{11} cm^{-3}, high velocity winds could transport H^+ and He^+ over several thousand kilometers, assisting the spread of H_3^+ to the mid-to-low latitudes.

5.2. Joule Heating

The relatively high level of H_3^+ emission might also be explained in part by the generation of energy as a result of joule heating, due to the frictional effect of ions horizontally accelerated by the electric field through the neutral atmosphere. Atreya (1986) estimates that the height-integrated Pedersen conductivity of the nonauroral jovian ionosphere is of the order of 0.2 mho, about 50 times less than its auroral counterpart. He also estimates the joule heating produced at auroral latitudes to be about 5 ergs s^{-1} cm^{-2}. Given the same electric field strength at both auroral and mid-to-low latitudes, one might therefore expect joule heating in the nonauroral latitudes to be of the order of 0.1 ergs s^{-1} cm^{-2}. This is likely, however, to be somewhat of an overestimate, since higher electric field strengths are expected in the auroral regions than at mid-to-low latitudes. Nonetheless, if this argument is correct, and if the level of joule heating were close to 0.1 ergs s^{-1} cm^{-2}, this mechanism could account for a fraction of the

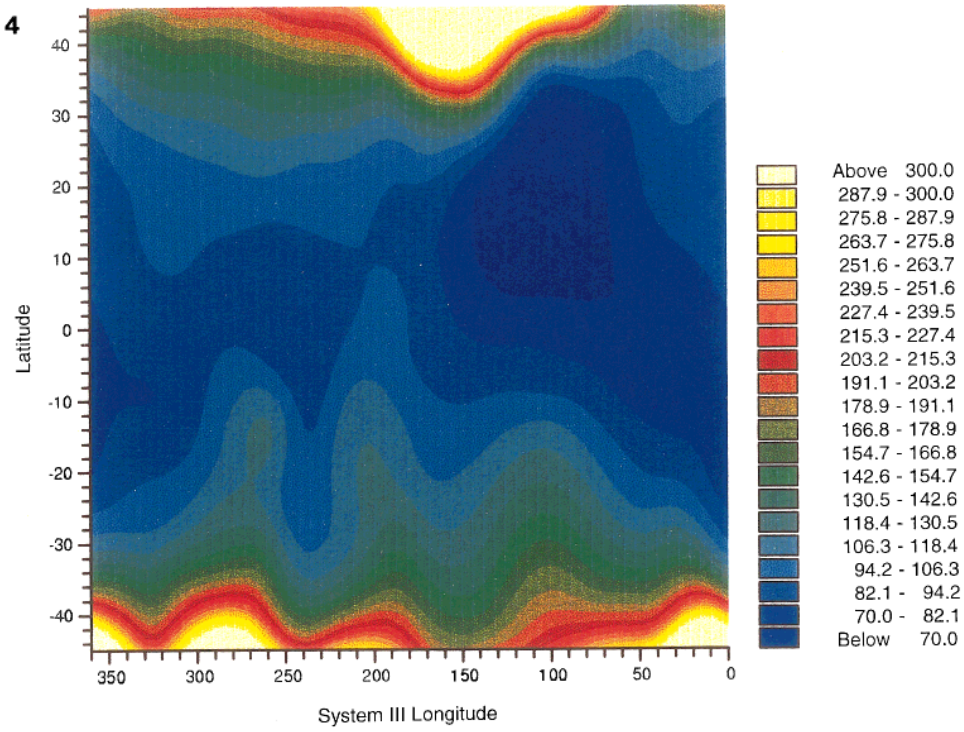
4
Latitude
System III Longitude
Above 300.0
287.9 - 300.0
275.8 - 287.9
263.7 - 275.8
251.6 - 263.7
239.5 - 251.6
227.4 - 239.5
215.3 - 227.4
203.2 - 215.3
191.1 - 203.2
178.9 - 191.1
166.8 - 178.9
154.7 - 166.8
142.6 - 154.7
130.5 - 142.6
118.4 - 130.5
106.3 - 118.4
94.2 - 106.3
82.1 - 94.2
70.0 - 82.1
Below 70.0

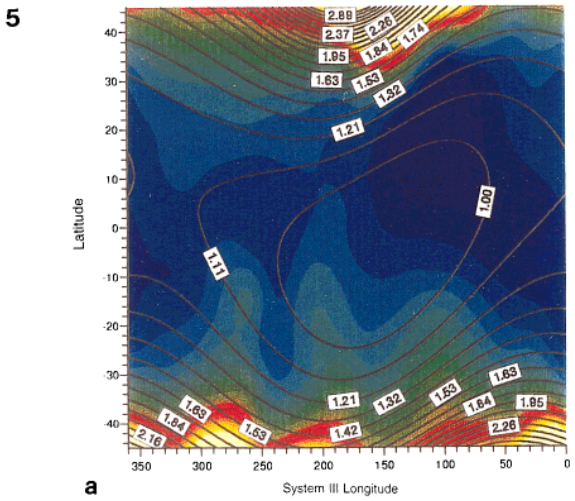
5
a
Latitude
System III Longitude

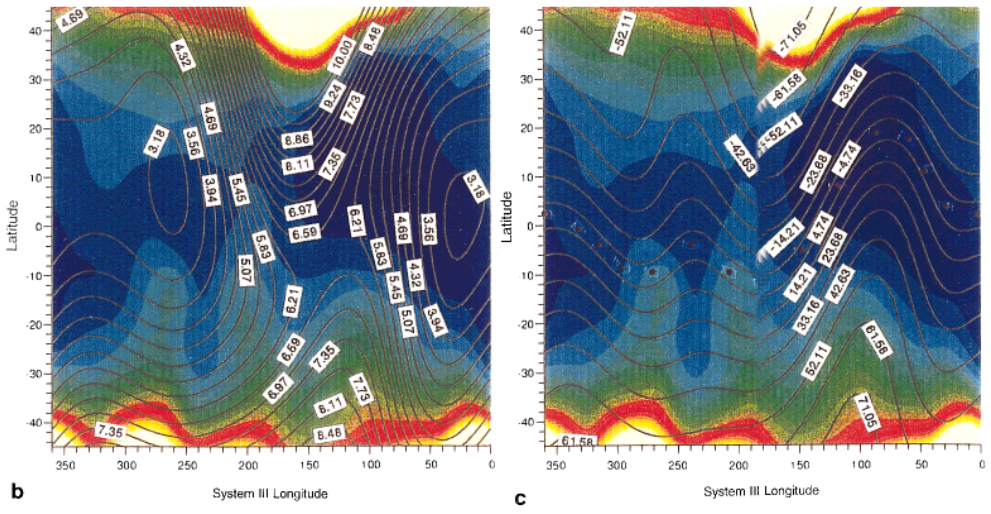
b
c
Latitude
System III Longitude

observed mid-to-low latitude H_3^+ energy output, depending on the efficiency with which it is assumed the energy from joule heating is converted into H_3^+ emission.

5.3. Particle Precipitation

The other most likely source of energy to produce the observed H_3^+ emission is particle precipitation. This mechanism has the advantage that it also identifies the source of the ionisation necessary to produce the ion. Precipitation of 1 to 10 keV electrons, with fluxes of around 1 to 10 ergs s^{-1} cm^{-2}, is usually invoked to explain the observed jovian auroral emission (e.g. Kim, Fox and Porter, 1992). The electrons are considered to originate mainly (i) from field aligned currents which follow magnetic field lines near the boundary between closed and open field lines, and (ii) from the pitch-angle scattering along magnetic field lines of particles residing in Jupiter's equatorial current sheet, with additional contributions, including some originating in the Io Plasma Torus.

Waite *et al.* (1997) have recently proposed that the X-ray emission from Jupiter's "near-equatorial" latitudes may result from energetic ion precipitation; their estimated requirement is 0.8 ergs s^{-1} cm^{-2} of sulfur and oxygen ions with energies above 300 keV/amu. Waite *et al.* (1997) also suggest that these ions can be supplied by precipitation from the inner radiation belt, which might also supply the keV electrons deemed necessary for H_3^+ production. Additionally, results from the energetic particle instrument (EPI) aboard the Galileo atmospheric probe indicate that there are high concentrations of energetic electrons extending all the way from the Io Plasma Torus to just 1.35 R_J, where their concentration appears to fall off abruptly (Fischer *et al.*, 1996), marking the inner boundary of the inner radiation belt in the jovian equatorial plane. Fischer *et al.* (1996) report that their electron flux profile is consistent with the measurements of Pioneer 11. The EPI results show that MeV electron fluxes are around 10^6 cm^{-2} sr^{-1} s^{-1} from 5 R_J to around 1.5 R_J, with a peak of nearly 10^7 cm^{-2} sr^{-1} s^{-1} around 2.2 R_J. Even though most of the particles detected by the EPI are trapped in radiation belts, the Galileo results still suggest that there may be supplies of keV electrons available to "leak" into the jovian atmosphere along field lines which correspond to the mid-to-low latitudes. The observed H_3^+ emission would require a total flux between 0.1 and 1.0 erg s^{-1} cm^{-2}, depending on the efficiency of ionisation and excitation. This flux is comparable to the input energy proposed by Atreya (1986) to account for the observed H_2 band intensities, as well as to the sulfur and oxygen ion fluxes required by Waite *et al.* (1997).

The scenario described above would appear to be consistent with the analysis of high resolution spectra of Jupiter's nonauroral regions obtained by Feldman *et al.* (1993) using the Hopkins Ultraviolet Telescope (HUT). Their study concluded that, of the slit-averaged emission rate of H Lyman-β of 2.3 kR cm^{-2}, only about 17–22% could be explained by solar induced fluorescence. They further concluded that photoelectrons could not account for the remainder of the emission and that other electron impact mechanisms were required to supply the energy required to explain the observations. Further analysis by Morrissey *et al.* (1995) broadly supported Feldman *et al.*'s (1993) interpretation. The conclusion that electron impact/precipitation is required to account for the observed UV emission has recently been challenged by Liu and Dalgarno (1996), however. These workers carried out detailed modelling of the HUT spectra and conclude that solar fluorescence could account for 57% of the observed emission, with photoelectrons supplying the rest of the energy without recourse to any other source of excitation.

If Liu and Dalgarno (1996) are correct, then there is no support for particle precipitation to be found in the HUT spectra. But their analysis may not be inconsistent with the mid-to-low-latitude H_3^+ emission being due in part to particle precipitation. Liu and Dalgarno derive a temperature of 530 K, placing the emission peak for H_2 molecules "above or within" the homopause, normally placed around the 1 μbar level. This conclusion is consistent with their requirement for moderate absorption of the emission by methane. But their analysis does not rule out precipitating particles penetrating to the 1 to 10 nanobar level where the peak H_3^+ production by solar EUV is predicted to occur (Kim *et al.*, 1992). In the auroral regions, precipitating keV electrons deposit most of their energy between 1 μbar and 100 nbar, just around the homopause, resulting in intense H_3^+ and atomic and molecular hydrogen emission. At lower latitudes, however, the dip angles of magnetic field lines are more shallow than in the auroral regions and particles following these field lines would indeed be expected to deposit their energy higher in the atmosphere than corresponding "auroral" electrons do, leading to H_3^+ emission, albeit with a lower intensity than in the aurorae. Moreover,

FIG. 4. Spatial distribution of the mid-to-low-latitude jovian H_3^+ emission, $E(H_3^+)$, in erg cm^{-2} s^{-1}. (Corrections for line of sight effects have been made.)

FIG. 5. Figure 4 overlaid with (a) footprints of the magnetic *l*-shells predicted by the Offset Tilted Dipole model of Acuña and Ness (1976); (b) contours of equal magnetic field strength; and (c) contours of constant dip angle. The dip equator is indicated by the line of dots. ((b) and (c) from Connerney, 1993).

entirely solar EUV produced H_3^+ would produce a "flat" latitudinal emission profile (prior to line-of-sight correction), to a first approximation, in contradiction to the observed concave profile.

6. COMPARISON OF $E(H_3^+)$ WITH MAGNETIC FIELD PARAMETERS

If the bulk of the ionisation/excitation energy implied by the observed H_3^+ emission were being provided by particle precipitation, one might expect the spatial variation of $E(H_3^+)$ to be sensitive to magnetic field parameters. In Fig. 5a, the H_3^+ emission parameter is shown overlaid with contours of the parameter which distinguished various "shells" of magnetic field lines according to the maximum distance they extend from Jupiter's magnetic centre according to the Offset–Tilted Dipole model of Acuña and Ness (1976). We shall call these *l*-shells, to distinguish them from the more usual L-shells which refer to distance from the gravitational centre of the planet. In making comparisons between the loci of the *l*-shells and the emission, it should be noted (i) that the values of l refer to the maximum distance of the field line from the location of the offset tilted dipole, and (ii) that the *l*-shells are projected onto the 0.6-bar planetary surface, whereas the ionospheric region of interest in this paper is about 1,000 km above this. As a result, (i) around $\lambda_{III} = 180°$ the field lines of any *l*-shell cross the magnetic equator about 0.1 R_J further from the gravitational center of the planet than the l number suggests, whereas around $\lambda_{III} = 0°$ it is about 0.1 R_J less; and (ii) all of the footprints at all longitudes should actually be moved to slightly higher latitudes. One point of note is that the footprint of $l = 1.35$ R_J only reaches down just below latitudes of $\pm 20°$ at some longitudes, while for others it is as high as 40°. Most of the brightest emission occurs at latitudes higher than the $l = 1.35$ R_J footprint, as far as our spatial resolution allows this to be determined, suggesting some correlation with the particle densities observed by the Galileo EPI. But levels of H_3^+ emission around 0.1 ergs s^{-1} cm^{-2} still exist all the way to the jovian equator, suggesting that populations of keV particles may exist inside the 1.35 R_J EPI cut-off for higher energy MeV electrons and positive ions.

In Fig. 5b, $E(H_3^+)$ is shown overlaid with the magnetic field strength predicted by Connerney's O6 model (Connerney, 1993). For any given latitude, there is a tendency for higher emissions to be associated with lower field strengths, as would be expected from diffuse particle precipitation. Similarly, if one traces footprints of constant l (from Fig. 5a) in the northern and southern hemispheres, for any longitude, there is also a tendency for H_3^+ emission to be higher in the hemisphere where the footprint of the *l*-shell in question encounters the lower field strength. Even more noticeable, however, is that the "warm channel" of the temperature and $E(H_3^+)$ map, around $\lambda_{III} = 170°$–$200°$, coincides with a region where westward-drifting (B-gradient curvature) electrons would notice a steeply decreasing magnetic field, lowering their mirror points and making precipitation into the atmosphere more likely (the "windshield wiper" effect). Conversely in the region between $\lambda_{III} = 50°$ and 150°, where westward-drifting electrons would encounter a rapidly increasing field, particularly in the northern hemisphere, H_3^+ emission is at a relative minimum.

There appears to be some additional correlation between the emission and the dip angle, shown in Fig. 5c. In particular, the minimum in the emission follows the dip equator quite closely, particular for $\lambda_{III} = 330°$ to 150°. This result might be explained considering that the depth to which precipitating particles of any given energy will penetrate will clearly depend on the angle at which they encounter the jovian atmosphere. Particles precipitating at steeper angles would be more likely to penetrate to deeper layers where concentrations of molecular hydrogen, and thus H_3^+ production rates, are higher.

7. CONCLUSIONS

The main conclusion of this study of the mid-to-low-latitude emission of H_3^+ is that this ion is responsible for a much greater cooling effect than previous modeling has allowed for. We also conclude that these relatively high values of $E(H_3^+)$ cannot be explained unless H_3^+ is being transported from the auroral regions and/or there is particle precipitation in the mid-to-low-latitude regions, as may be necessary for the observed X-ray emission (Waite *et al.*, 1997). The latter explanation, if correct, would suggest that particles with energies in the keV domain populate the space between the Galileo EPI cutoff at 1.35 R_J and the planet itself. Future models of the jovian ionosphere should therefore take account of these effects. This and subsequent work (Miller *et al.*, work in progress) suggests that for the mid-to-low latitudes temporal fluctuations on timescales of a few days are relatively minor. In the future, therefore, we feel that spectroscopic studies of jovian H_3^+ emission such as the one presented here will be of great assistance in models of the non-auroral ionosphere, and in investigating links to magnetic field parameters and circulatory phenomena.

ACKNOWLEDGMENTS

It is a pleasure to acknowledge the expert assistance of the staff at UKIRT, which is operated by the Joint Astronomy Centre, Hilo, on behalf of the U.K. Particle Physics and Astronomy Research Council (PPARC). PPARC is also thanked for the award of a Ph.D. studentship to HAL, and for Grant GR/K97837, which funded much of this work. This paper has benefitted considerably from the comments of the two

referees: Dr. Sang J. Kim brought our attention to potential contaminants in the jovian reflected solar spectrum; an anonymous referee helped clarify our comparison of H_3^+ emission with magnetic field parameters. Special thanks are also due to Prof. Renée Prangé for her advice and assistance during the preparation of this paper and Paper II. We also express our appreciation to Drs. Daniel Rego, J. Hunter Waite, Jr., and Brian Mitchell for helpful discussion during the preparation of this manuscript.

Note added in proof. It has been drawn to our attention that the vertical scale in Figs. 8a and 8b of Paper II should be divided by 3.

REFERENCES

Achilleos, N., S. Miller, J. Tennyson, A. Aylward, and D. Rees, 1997. JIM: Time-dependent, three-dimensional modelling of Jupiter's thermosphere. *J. Geophys. Res*., submitted.

Acuña, M. H., and N. F. Ness 1976. The main magnetic field of Jupiter. *J. Geophys. Res.* **81,** 2917–2922.

Atreya, S. K. 1986. Atmospheres and ionospheres of the outer planets and their satellites, pp. 139–143. Springer-Verlag, Heidelberg.

Atreya, S. K., and T. M. Donahue 1976. Model ionospheres of Jupiter. In *Jupiter* (T. Gehrels, Ed.), pp. 304–310. Univ. of Arizona Press, Tucson.

Ballester, G. E., S. Miller, J. Tennyson, T. R. Geballe, and L. M. Trafton 1994. Latitudinal temperature variations of jovian H_3^+. *Icarus* **107,** 189–194.

Ben Jaffel, L., J. T. Clarke, R. Prangé, G. R. Gladstone, and A. Vidal-Madjar 1992. A new model for the Lyman alpha bulge of Jupiter. *Geophys. Res. Lett.* **20,** 747–750.

De Bergh, C., A. Martin., T. Owen, D. Gautier, J.-P. Maillard, B. L. Lutz, and P. Drossart 1992. Paper presented at workshop on variable phenomena in jovian planetary systems, Annapolis, MD.

Clarke, J. T., and 19 co-authors 1995. HST far-ultraviolet imaging of Jupiter during the impacts of Comet Shoemaker–Levy-9. *Science* **267,** 1302–1307.

Connerney, J. E. P. 1993. Magnetic fields of the outer planets. *J. Geophys. Res.* **98,** 18,659–18,679.

Dinelli, B. M., S. Miller, N. Achilleos, H. A. Lam, M. Cahill, J. Tennyson, M.-F. Jagod, T. Oka, J.-C. Helico, and T. R. Geballe 1997. UKIRT observations of the impact and consequences of Comet Shoemaker–Levy 9 on Jupiter. *Icarus* **126,** 107–125.

Drossart, P., J-P. Maillard, J. Caldwell, S. J. Kim, J. K. G. Watson, W. A. Majewski, J. Tennyson, S. Miller, S. K. Atreya, J. T. Clarke, J. H. Waite, Jr., and R. Wagener 1989. Detection of H_3^+ on Jupiter. *Nature* **340,** 539–541.

Feldman, P. D., M. A. McGrath, H. W. Moos, S. T. Durrance, D. F. Strobel, and A. F. Davidsen 1993. The spectrum of the jovian dayglow observed at 3A resolution with the Hopkins Ultraviolet Telescope. *Astrophys. J.* **406,** 279–284.

Fischer, H. M., E. Pehlke, G. Wibberbez, L. J. Lanzerotti, and J. D. Mihalov 1996. High-energy charged particles in the innermost jovian magnetosphere. *Science* **272,** 856–858.

Hamilton, D. C., G. Gloeker, S. M. Krimigis, C. O. Bostrom, T. P. Armstrong, W. I. Axford, C. Y. Fan, L. J. Lanzerotti, and D. M. Hunten 1980. Detection of energetic hydrogen molecules in Jupiter's magnetosphere by Voyager 2: Evidence for an ionic plasma source. *Geophys. Res. Lett.* **7,** 813–816.

Kim, Y. H., J. L. Fox, and H. S. Porter 1992. Densities and vibrational distribution of H_3^+ in the jovian auroral ionosphere. *J.Geophys. Res.* **97,** 6093–6101.

Kim, S. J., G. S. Orton, C. Dumas, and Y. H. Kim 1996. Infrared spectroscopy of Jupiter's atmosphere after the A and E impacts of Comet Shoemaker–Levy 9. *Icarus* **120,** 326–331.

Lam, H. A. 1995. Monitoring the jovian ionosphere using H_3^+ emission as a probe. *Ph.D. thesis*, University of London.

Lam, H. A., N. Achilleos, S. Miller, J. Tennyson, L. M. Trafton, T. R. Geballe, and G. E. Ballester 1997. A baseline spectroscopic study of the infrared aurorae of Jupiter. *Icarus* **127,** 379–393.

Lean, J. 1987. Solar ultraviolet irradiance variations: A review, *J. Geophys. Res.* **92,** 839–868.

Liu, W., and A. Dalgarno 1996. The ultraviolet spectrum of the jovian dayglow. *Astrophys. J.* **462,** 502–518.

Livingstone, W., and L. Wallace 1994. *An Atlas of the Solar Spectrum in the Infrared from 1850 to 9000 cm*$^{-1}$ (*1.1 to 5.4* μm). National Solar Observatory Technical Report.

McConnell, J. C., and T. Majeed 1991. H_3^+ in the jovian ionosphere. *J. Geophys. Res.* **92,** 8570–8578.

Miller, S., T. R. Geballe, L. M. Trafton, G. E. Ballester, and J. Tennyson 1992. H_3^+ distribution on Jupiter. *Bull. Am. Astron. Soc.* **24,** 1034–1035.

Miller, S., H. A. Lam, and J. Tennyson 1994. What astronomy has learned from H_3^+. *Can. J. Phys.* **72,** 760–771.

Miller, S., and 12 other authors, 1995. The effect of the impact of Comet Shoemaker–Levy 9 on Jupiter's aurorae. *Geophys. Res. Lett.* **22,** 1629–1623.

Mitchell, J. B. A. 1990. The dissociative recombination of molecular ions. *Phys. Rep.* **186,** 215–248.

Morrissey, P. F., P. D. Feldman, M. A. McGrath, B. C. Wolves, and H. W. Moos 1995. The ultraviolet reflectivity of Jupiter at 3.5A resolution from Astro-1 and Astro-2. *Astrophys. J.* **454,** L65–L68.

Prangé, R., D. Rego, L. Pallier, L. Ben Jaffel, C. Emerich, J. T. Clarke, G. E. Ballester, and J. Ajello 1997. Detection of self-reversed Lyman-α lines from the jovian aurorae with the Hubble Space Telescope. *Astrophys J.*, in press.

Rego, D., R. Prangé, and J. C. Gerard, 1994. Auroral Lyman-α and H_2 bands from the giant planets. 1. Excitation by proton precipitation in the jovian atmosphere, *J. Geophys. Res. Planets* **99,** 17,075–17,094.

Roberge, W., and A. Dalgarno 1982. The formation and destruction of HeH+ in astrophysical plasmas. *Astrophys. J.* **255,** 489–496.

Schultz, R., Th. Encrenaz, J. Stuwe, and G. Wiederman 1995. Monitoring the near-i.r. emission features at the NTT and detection of the northern counterparts. In *Proc. Euro. SL9/Jupiter Workshop, 1995* (R. West and H. Bohnhardt, Eds.), pp. 363–368.

Sommeria, J., L. Ben Jaffel, and R. Prangé 1995. On the existence of supersonic jets in the upper atmosphere of Jupiter. *Icarus* **119,** 2–25.

Strobel, D., and S. Atreya 1983. Ionosphere. In *Physics of the Jovian Magnetosphere* (A. Dessler, Ed.), p. 57. Cambridge Univ. Press, Cambridge, UK.

Waite, J. H., Jr., T. E. Cravens, J. U. Kozyra, A. F. Nagy, S. K. Atreya, and R. H. Chen 1983. Electron precipitation and related aeronomy of the jovian thermosphere and ionosphere. *J. Geophys. Res.* **88,** 6143–6163.

Waite, J. H., Jr., G. R. Gladstone, P. Drossart, T. E. Cravens, A. Maurellis, W. S. Lewis, B. Mauk, and S. Miller 1997. Jovian equatorial X-ray emission: Key to understanding high atmosphere temperatures measured by the Galileo probe. *Science* **276,** 104–108.